$LiNbO_3$ ground- and excited-state properties from first-principles calculations

W. G. Schmidt,* M. Albrecht, S. Wippermann, S. Blankenburg, and E. Rauls
Lehrstuhl für Theoretische Physik, Universität Paderborn, 33095 Paderborn, Germany

F. Fuchs, C. Rödl, and J. Furthmüller
Institut für Festkörpertheorie und -optik, Friedrich-Schiller-Universität, Max-Wien-Platz 1, 07743 Jena, Germany

A. Hermann
Centre of Theoretical Chemistry and Physics, The Institute for Advanced Study, Institute of Fundamental Sciences, Massey University, Private Bag 102904, North Shore MSC, Auckland, New Zealand

(Received 1 October 2007; revised manuscript received 22 November 2007; published 3 January 2008)

The atomic and electronic structure, zone center phonon frequencies, and optical absorption of $LiNbO_3$ are calculated from first principles. The structural and vibrational properties predicted from density functional theory are in good agreement with experiment and earlier theoretical work. The electronic band-structure and optical properties are found to be very sensitive to quasiparticle and electron-hole attraction effects, which are included here using the *GW* approach and by solving the Bethe-Salpeter equation, respectively. We predict the fundamental gap to be more than 1 eV larger than the 3.7 eV frequently cited for ferrolectric $LiNbO_3$ and calculate optical absorption spectra in good agreement with experiment.

DOI: 10.1103/PhysRevB.77.035106 PACS number(s): 71.15.Mb, 71.15.Qe, 71.35.Cc

The electro-optic, photorefractive, and nonlinear optical properties of lithium niobate ($LiNbO_3$, LN) are exploited in a number of devices such as modulators for fiber-optic communications systems or holographic applications. LN, see Refs. 1 and 2 for tutorial papers on its physical properties, occurs in two phases of trigonal symmetry with ten atoms per unit cell, (see Fig. 1). The ground state is ferroelectric with space group $R3c$. The high-symmetric paraelectric phase with space group $R\bar{3}c$ is stable above 1480 K.

Given the vast range of LN applications, our knowledge about its electronic and optical properties is surprisingly limited. For example, we are not aware of a measured band structure. The direct band gap of 3.78 eV for the ferroelectric phase—frequently cited in the literature—is actually concluded from optical experiments.[3] Therefore, it is affected by electron-hole attraction effects which may reduce the size of the actual band gap, i.e., the difference between the ionization energy and the electron affinity, substantially.[4–7] The situation is additionally complicated by the fact that there are actually a number of band gap values reported, all concluded from optical absorption experiments. They range from the indirect gap of 3.28 eV reported in Ref. 8 to values of 4.0 or 4.3 eV.[9,10] The optical absorption experiments mentioned above as well as further studies, e.g., Ref. 11, focus mainly on the onset of the absorption. We are aware of only two studies that address the absorption in the vacuum ultraviolet (VUV) domain.[12,13] The lack of experimental data may partially be related to the fact that the crystal growing process results in samples that are not stoichiometric, but Li deficient. In fact, many LN applications depend on intentional impurities of the material. Moreover, the paraelectric phase is stable in a small temperature window only.

However, the theoretical understanding is also limited. There are now a number of first-principles studies available on the LN structural and vibrational properties (see, e.g., Refs. 14–16) that basically explain the measured phonon modes. Also, the phase transition between para- and ferroelectric LN was modeled with molecular dynamics.[17] Only few calculations, however, address the optical and electronic properties. Most first-principles band-structure calculations, e.g., Refs. 15 and 18, are based on a single-particle picture and neglect quasiparticle effects that typically widen the band gap between occupied and empty states by a large fraction of its value.[19] The seemingly good agreement between measured and calculated band gaps for LN may therefore result from a fortuitous error cancellation between the possibly large exciton binding energy and the electronic self-energy. An early theoretical study by Ching *et al.*[20] indicated the importance of self-energy effects: Using the approximate Sterne-Inkson model,[21] they predicted self-energy corrections of the order of 1 eV. However, the single-particle gap in Ref. 20 is much smaller (2.62 eV for the ferroelectric phase) than in the more recent studies, (3.69 eV) (Ref. 18) and (3.48 eV).[15] To our knowledge, the influence of excitonic and local-field effects on the optical absorption is completely unknown. Existing studies on the optical absorption rest on the single-(quasi)particle approximation and predict broad ($\sim$1–2 eV) absorption peaks centered at or below 5 and 9 or 7 eV, respectively,[18,20] i.e., below the measured absorption peak positions.[12,13]

The better understanding of the LN ground- and, in particular, excited-state properties is the aim of the present study. Thereby, we proceed in three steps. (i) We use density functional theory in generalized gradient approximation (DFT-GGA) to determine the structurally relaxed ground state of both the ferro- and paraelectric LN phases. The reliability of our scheme is demonstrated by comparing the structural and vibrational properties with earlier theoretical data and experiment. The phonon modes and frequencies are calculated using the frozen-phonon approach.[22] This approach does not include the long-range electric fields that accompany longitudinal phonons. For this reason, we restrict ourselves to the transverse modes. DFT-GGA also provides the Kohn-Sham eigenvalues and eigenfunctions that enter the

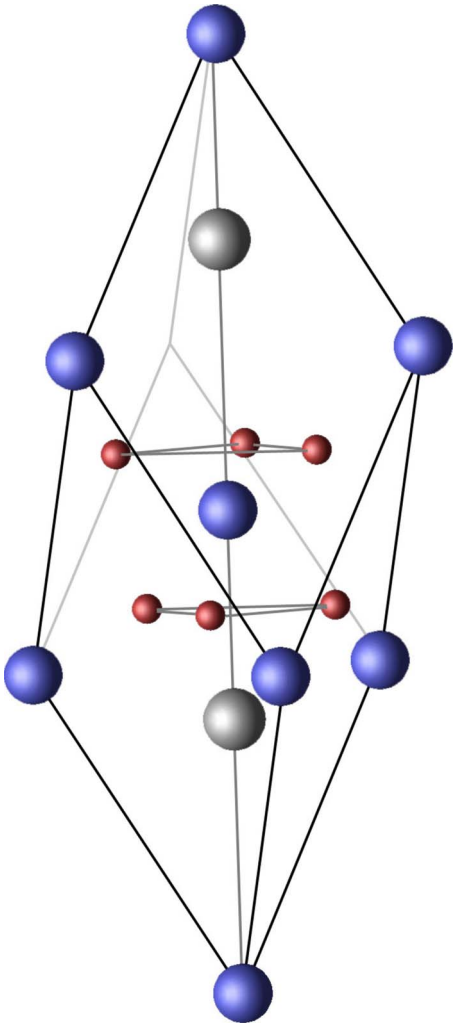

FIG. 1. (Color online) Primitive unit cell of the ferroelectric phase of LN. Light, small, and dark balls indicate the positions of Li, O, and Nb, respectively.

single- and two-particle Green's functions. (ii) The the electronic quasiparticle spectrum is obtained within the *GW* approximation (GWA)[23] to the exchange-correlation self-energy, and finally (iii) the Bethe-Salpeter equation (BSE) is solved for coupled electron-hole excitations,[4–6] thereby accounting for the screened electron-hole attraction and the unscreened electron-hole exchange.[24–26]

In detail, we start from first-principles projector augmented wave calculations using the VASP implementation of the DFT-GGA.[27,28] A $4\times4\times4$ **k**-point mesh is used to sample the Brillouin zone. The electron wave functions are expanded into plane waves up to an energy cutoff of 400 eV. The mean-field effects of exchange and correlation in GGA are modeled using the PW91 functional.[29] In the second step, we include electronic self-energy effects, i.e., replace the GGA exchange and correlation potential by the nonlocal and energy-dependent self-energy operator $\Sigma(\mathbf{r},\mathbf{r}';E)$. We calculate Σ in the *GW* approximation[23] from the convolution of the single-particle propagator G and the dynamically screened Coulomb interaction W. As a further approximation, we use a model dielectric function[30] to calculate W. Thereby, the wave-vector (**q**) dependence of the dielectric function is given by

$$\epsilon(\mathbf{q},\rho) = 1 + \left[\frac{1}{\epsilon_\infty - 1} + \left(\frac{q}{q_{TF}(\rho)}\right)^2 + \frac{3q^4}{4k_F^2(\rho)q_{TF}^2(\rho)}\right]^{-1}, \tag{1}$$

where k_F and q_{TF} represent the Fermi and Thomas-Fermi wave vectors, respectively, which depend on the electron density ρ. This expression interpolates between the correct behaviors at high and low **q** vectors and, by construction, correctly obtains the dielectric constant for $\mathbf{q}=0$. Using this model, screening speeds up the calculations substantially and results in quasiparticle shifts that are typically accurate within about 10% of the complete calculations.[31,32] The electron-hole interaction is taken into account in the third step. The two-particle Hamiltonian,

$$\begin{aligned} H_{vc\mathbf{k},v'c'\mathbf{k}'} = {} & (\epsilon_{c\mathbf{k}} - \epsilon_{v\mathbf{k}})\delta_{vv'}\delta_{cc'}\delta_{\mathbf{k},\mathbf{k}'} + 2\int\int d\mathbf{r}d\mathbf{r}'\psi^*_{c\mathbf{k}}(\mathbf{r}) \\ & \times \psi_{v\mathbf{k}}(\mathbf{r})\bar{v}(\mathbf{r}-\mathbf{r}')\psi_{c'\mathbf{k}'}(\mathbf{r}')\psi^*_{v'\mathbf{k}'}(\mathbf{r}') \\ & - \int\int d\mathbf{r}d\mathbf{r}'\psi^*_{c\mathbf{k}}(\mathbf{r})\psi_{c'\mathbf{k}'}(\mathbf{r})W(\mathbf{r},\mathbf{r}') \\ & \times \psi_{v\mathbf{k}}(\mathbf{r}')\psi^*_{v'\mathbf{k}'}(\mathbf{r}'), \end{aligned} \tag{2}$$

describes the interaction of pairs of electrons in conduction states $|c\mathbf{k}\rangle$ and holes in valence states $|v\mathbf{k}\rangle$.[24–26] The diagonal first part is given by the quasiparticle energies obtained in *GW* approximation. The second, the electron-hole exchange term, where the short-range part of the bare Coulomb potential $\bar{v}$ enters, reflects the influence of local fields. Finally, the third part, which describes the screened electron-hole attraction, is calculated using the same approximations for W as in the self-energy. For the actual calculation of the polarizability, we use the time-evolution implementation described in Refs. 32 and 33.

The relaxed ground-state geometries for ferro- and paraelectric LN are the starting points for all further investigations. In paraelectric LN, the Li and Nb atoms are at Wyckoff positions 6a and 6b (hexagonal axes), respectively, while the O atoms are located at 18e, with internal parameter x. We determine lattice constants $a=5.219$ Å, $c=13.756$ Å, and $x=0.041$. The measured values amount to 5.289 Å, 13.848 Å, and $x=0.06$.[34] The usage of GGA often leads to a slight overestimation of lattice constants. The fact that an underestimation of about 1% occurs here may be related to the thermal expansion of the sample—the paralelectric phase is stable for temperatures above 1480 K—which is not included in our ground-state calculations. Earlier GGA results[15] are, in fact, quite similar to our findings: $a=5.255$ Å, $c=13.791$ Å, and $x=0.048$.

In ferroelectric LN, Li and Nb are located at Wyckoff position 6a (hexagonal axes) with internal parameter z_{Nb}; oxygen atoms are at 18b with parameters u, v, and w. Following the notation in Ref. 15, we determine $a=5.161$ Å, $c=13.901$ Å, $z_{\mathrm{Nb}}=0.0339$, $u=0.012\,05$, $v=0.0278$, and $w=0.0191$. The deviation from experiment[34] ($a=5.151$ Å, c

TABLE I. Calculated phonon frequencies (in cm^{-1}) of transverse E and A_1 as well as A_2 modes of ferroelectric LN in comparison with measured data from Refs. 36–43.

	Present	Measured
A_1	238	251–252
	279	273–276
	350	331–333
	605	631–634
A_2	212	224
	298	314
	406	
	443	455
	868	
E	147	152–155
	216	177–180
	260	236–238
	321	321–325
	384	370–371
	421	431–436
	573	579–586
	662	686–670

$=13.876$ Å, $z_{Nb}=0.0329$, $u=0.00947$, $v=0.0383$, and $w=0.0192$) is much smaller than for the paraelectric phase, corroborating our assumption that thermal expansion may be responsible for much of the deviation in the paraelectric case. Again, close agreement with the GGA results of Veithen and Ghosez is observed.[15]

The calculated energy difference between the para- and ferroelectric LN phases amounts to 0.30 eV and is thus of similar magnitude as found in full potential linearized augmented plane-wave calculations that predicted 0.25 eV.[35]

The calculation of phonon frequencies is another sensitive test for the accuracy of our approach. From calculations with and without symmetry constraints as well as by using different magnitudes for the frozen deformations, we find the *numerical* accuracy of the frozen-phonon approach used to depend strongly on the specific mode. For most modes, however, the numerical error bar is below 10 cm^{-1}. There are a number of experimental studies of the ferroelectric LN dynamical properties available. At the Γ point, the optical phonons can be classified according to the irreducible representations of the space group $R3c$ into A_1, A_2, and E modes. In Table I, we assign our results to the experimental findings for the respective transverse E and A_1 modes as well as A_2 phonons. Within deviations of at most 36, but typically about 10 cm^{-1}, the calculated frequencies match the experimental findings. The accuracy of our calculations is thus comparable to earlier frozen-phonon calculations,[14] but somewhat inferior to linear-response calculations[15] that are less sensitive to anharmonicities than the present approach. Two A_2 modes at around 400 and 900 cm^{-1} are predicted here as well as in earlier calculations,[14,15] but have not been detected yet.

TABLE II. Calculated phonon frequencies (in cm^{-1}) of A_{1g}, A_{1u}, A_{2g}, and E_g as well as transverse A_{2u} and E_u modes of paraelectric LN in comparison with earlier calculations (Ref. 15).

	Present	Earlier theory
A_{1g}	406	403
A_{1u}	283	279
	432	435
A_{2g}	$92i$	$115i$
	410	405
	868	889
E_g	204	175
	436	425
	481	501
	578	589
A_{2u}	$183i$	$201i$
	47	94
	476	478
E_u	18	$53i$
	207	177
	384	393
	443	460
	533	532

We are not aware of measured phonon frequencies for paraelectric LN. Therefore, we present in Table II a comparison with the linear-response results from Veithen and Ghosez.[15] The data are classified according to the irreducible representations of the space group $R\bar{3}c$. As can be seen, the agreement is of similar quality as discussed above for ferroelectric LN. The largest deviation concerns the lowest E_u mode that is unstable according to Ref. 15, but stable here. We mention that this mode was also identified as stable by Parlinski *et al.*[16] As discussed in Ref. 15, the low energy of this mode makes it susceptible to numerical errors.

The results above indicate good agreement between the DFT-GGA calculations and experiment concerning the structural ground state as well as vibrational properties of LN. On this basis, we can start to analyze the electronic properties. In Fig. 2, we plot the Kohn-Sham energies along high symmetry lines of the hexagonal Brillouin zone (cf. Fig. 3) of ferro- and paraelectric LN. Within the single-particle approximation, the ferro- and paraelectric phases have indirect band gaps of 3.48 and 2.47 eV, respectively. These values agree well with other recent DFT calculations,[15] which predict 3.50 and 2.51 eV, respectively. The valence-band maximum (VBM) occurs at the Γ point for both phases, while the conduction-band minima (CBM) are located at $0.4\Gamma-K$ and the K point for the ferro- and paraelectric phases, respectively.

The character of the electronic states forming the VBM and the CBM is shown in Fig. 4. As can be seen, the VBM is

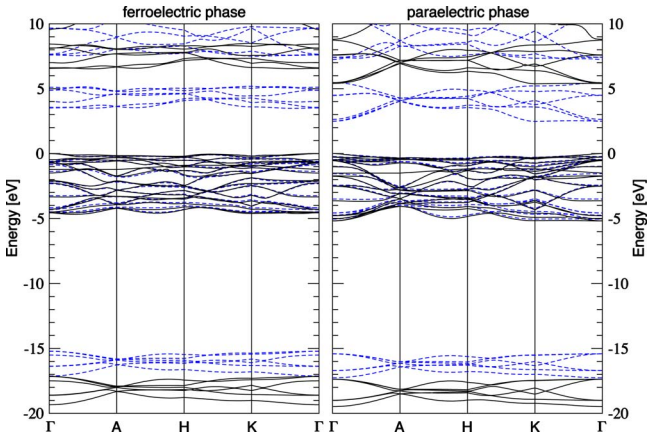

FIG. 2. (Color online) Calculated band structures of ferro- (left) and paraelectric LN (right) calculated within the DFT-GGA (dashed lines) and the *GW* approximation (solid lines).

formed by O $2p$ states, whereas the Nb $4d$ states form the CBM. The low lying energy band is formed by O $2s$ states, not shown here.

The band gap calculated within DFT-GGA does not correspond to the optical gap measured experimentally, since neither electronic quasiparticle, i.e., self-energy, effects nor electron-hole attraction, i.e., excitonic effects, is included. In order to estimate the size of quasiparticle effects in LN, we perform *GW* calculations for both the ferroelectric and paraelectric phases. The correspondingly corrected energy bands are shown with solid lines in Fig. 2. Obviously, the band gap is opened substantially, by about 3 eV. Also, the dispersion changes slightly. For example, the CBM of the ferroelectric phase changes from $0.4\Gamma-K$ to $0.6\Gamma-A$. The—thus still indirect—band gap amounts to 6.53 eV. No change of the CBM position occurs for the paraelectric phase upon inclusion of quasiparticle effects. The indirect gap between Γ and K amounts now to 5.37 eV. However, both within DFT-GGA and the GWA, we find the lowest conduction band to be very flat around Γ for both phases. Therefore, the material can be regarded as having approximately a direct band gap at the Γ point.

The quasiparticle shifts obtained in our study are larger than previous results based on the Sterne-Inkson approach.[20] This may be related to the different electronic ground states

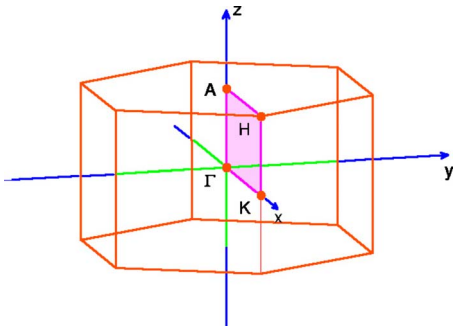

FIG. 3. (Color online) Notation of high symmetry Brillouin zone points used in the present work.

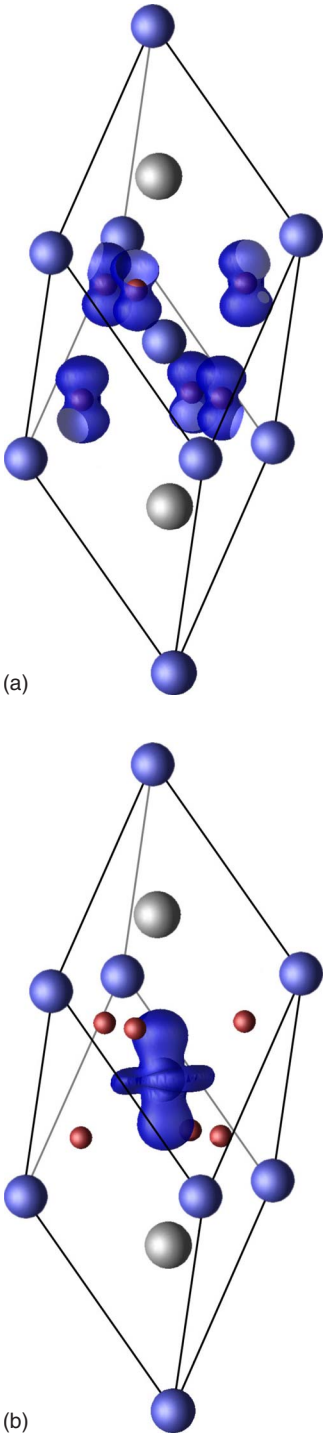

FIG. 4. (Color online) Orbital character of states of paraelectric LN near Γ for the VBM (left) and the CBM (right).

in both studies. Ching *et al.*[20] started from a band gap that is about 1 eV smaller than in the present work. The Sterne-Inkson approach itself may be another reason for the difference. It describes the inherently nonlocal self-energy operator by a local potential. On the other hand, the present calculations rest on a model dielectric function and the single plasmon-pole approximation,[30] which can also be expected to impair the accuracy.

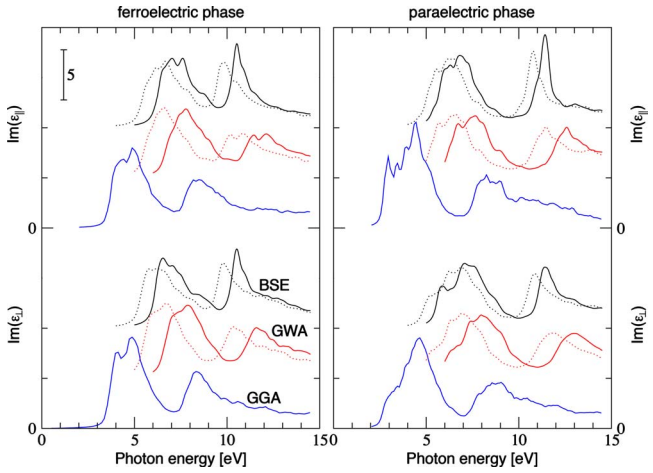

FIG. 5. (Color online) Imaginary part of the dielectric function of ferro- and paraelectric LN calculated within the DFT-GGA, the GWA, and from the BSE. Solid and dotted lines indicate the results if pure electronic screening and electronic screening plus lattice polarizability, respectively, are taken into account in the GWA and BSE calcuations (see text).

The single-particle excitations are accompanied by the rearrangement of the remaining electrons in the solid, which screen the excited electrons (above the Fermi level) and excited holes (missing electrons below the Fermi level). Polar materials such as LN, however, feature longitudinal optical phonons that give rise to macroscopic electric fields that couple to the excited electrons and holes and modify their motion. It can be expected that the lattice polarizability contributes to the dressing of the quasiparticles. This effect is not included in the GWA band structures shown in Fig. 2, which rest on the assumption of a pure electronic screening. To study the effect of the lattice polarizability on the single-particle excitation energies, in principle, the electron-phonon coupling needs to be considered. As discussed by Bechstedt *et al.*,[44] however, the *GW* approximation in conjunction with a model dielectric function[30] suggests a simple way to estimate the magnitude of possible effects due to the lattice polarizability. To this end, one modifies the modeling of the screening. Rather than using ϵ_∞ for the pure electronic screening, one considers to some extent also the contribution of the lattice polarizability $\sim(\epsilon_0-\epsilon_\infty)$. In the case of LN, where the static dielectric constant ϵ_0 is nearly 1 order of magnitude larger than the optical dielectric constant ϵ_∞ ($\sim$40 rather than $\sim$5),[45,46] large effects may be expected. If we assume a partial lattice contribution to the screening, and consider a dielectric constant of 20, we obtain quasiparticle shifts that are about half the size obtained for a pure electronic screening. Thus, the band gap of ferroelectric LN assumes a value of 5.37 eV, while we obtain 4.39 eV for paraelectric LN. While we are not aware of an experimental study devoted to the fundamental gap, from the theory point of view, we would thus expect a band gap between about 5.4 and 6.5 eV for ferroelectric LN and a value for paralectric LN that will be roughly 1 eV smaller.

In Fig. 5, we show the optical spectra calculated for ferro- and paraelectric LN according to the three levels of theory: i.e., DFT-GGA, GWA, and BSE. Again, it is not clear whether or not and to which extent the lattice polarizability plays a role on the time scale of the formation of Coulomb correlated electron-hole pairs.[44] In order to estimate the size of possible lattice effects, we proceed in a similar manner as discussed above for the GWA (cf. Ref. 44). We present calculations where pure electronic screening is taken into account (solid lines) as well as calculations where a partial lattice contribution is allowed for in the quasiparticle energies and the screened electron-hole attraction entering the two-particle Hamiltonian (2). The latter results are shown by dotted lines.

The spectrum obtained within DFT-GGA for ferroelectric LN agrees roughly with earlier independent-particle results.[18,20] There are two main features of the optical absorption centered at about 5 and 8 eV. They arise from transitions between O $2p$ and Nb $4d$ states see (Fig. 4). The inclusion of the many-body electron-electron interaction in GWA, i.e., the electronic self-energy, leads to a nearly rigid blueshift of the spectra by about 1.5–3 eV, depending on the screening. The Coulomb correlation of electrons and holes, accounted for by solving the BSE, changes the line shape somewhat. The first peak (or shoulder) of the low-energy main feature of the optical absorption becomes more pronounced, and the whole feature is redshifted compared to the GWA spectrum. It is now positioned at about 5.5 or 6.5 eV, depending whether or not a partial contribution of the lattice polarization is taken into account. The oscillator strength of the originally rather broad ($\sim$2 eV) high-energy main feature of the optical absorption is redshifted and transferred into a single sharp peak at about 9.5 or 10.5 eV, respectively. Similar changes occur for paraelectric LN.

Compared to the experimental data for the ferroelectric LN, where absorption peaks at 5.3–6 and 9.2–10 eV are observed,[12,13] the inclusion of self-energy and excitonic effects improves the theoretical description substantially. This concerns both the peak positions and the line shapes, which sharpen due to the inclusion of excitonic effects. Interestingly, the experimental observation that the first absorption peak is broader for $\epsilon_\parallel$ than for $\epsilon_\perp$ in ferroelectric material[13] is reproduced in the calculations that account for electron-hole interactions much more clearly than on the single-particle level of theory.

A precise comparison of our calculated spectra with experiment should, in principle, allow conclusions on the actual role played by the lattice in the screening of the Coulomb correlated electron-hole pairs. Unfortunately, such a comparison is hindered by the fact that the two existing measurements do not exactly agree on the positions of the absorption peaks. The more recent data of Mamedov *et al.*[12] indicated excitation energies that are about 0.7 eV larger than obtained by Wiesendanger and Günterodt.[13] The absorption peaks calculated at the BSE level of theory without lattice polarizability, however, are blueshifted with respect to both sets of experimental data. In contrast, the calculations where a partial contribution of the lattice to the screening is considered result in peak positions that lie within the respective lower and upper experimental data. This is no strict evidence for an actual influence of the lattice on the screening because (i) our method of calculation is approximate as dis-

cussed above and (ii) the experimental data themselves scatter. However, the experiment-theory comparison at least indicates that the lattice polarizability influences, in fact, to some extent the single- and two-particle electronic excitations in LN. Concerning the fundamental band gap, this means that a value around 5.3 eV for ferroelectric LN appears more likely than the 6.5 eV calculated without lattice contribution to the screening. In order to thoroughly understand the LN electronic and optical properties, detailed measurements of the band structure and the optical absorption of single, stoichiometric crystals, in particular, in the VUV region, would be most helpful.

To summarize, we performed first-principles calculations of the structural, vibrational, electronic, and optical properties of $LiNbO_3$. The ground-state structures and phonon frequencies calculated in the present work agree well with experiment and earlier *ab initio* theory. Also, the DFT-GGA band structure, i.e., the Kohn-Sham eigenvalues, agrees well with similar calculations performed earlier. However, our study indicates that the surprisingly good agreement of the Kohn-Sham gap with experiment stated often in the literature is fortuitous. Quasiparticle effects widen the band gap drastically beyond its DFT value. We predict values of 5.4–6.5 and 4.4–5.4 eV for ferro- and paraelectric LN. On the other hand, strong excitonic effects with exciton binding energies of the order of 1 eV can be expected.

We thank Wolfgang Sohler and Hubertus Suche for suggesting this work and very helpful discussions. The calculations were done using grants of computer time from the Paderborn Center for Parallel Computing (PC^2) and the Höchstleistungs-Rechenzentrum Stuttgart. The Deutsche Forschungsgemeinschaft is acknowledged for financial support.

*w.g.schmidt@upb.de

[1] A. Räuber, Curr. Top. Mater. Sci. **3**, 481 (1978).
[2] R. S. Weis and T. K. Gaylord, Appl. Phys. A: Solids Surf. **37**, 191 (1985).
[3] A. Dhar and A. Mansingh, J. Appl. Phys. **68**, 5804 (1990).
[4] S. Albrecht, L. Reining, R. Del Sole, and G. Onida, Phys. Rev. Lett. **80**, 4510 (1998).
[5] L. X. Benedict, E. L. Shirley, and R. B. Bohn, Phys. Rev. Lett. **80**, 4514 (1998).
[6] M. Rohlfing and S. G. Louie, Phys. Rev. Lett. **83**, 856 (1999).
[7] P. H. Hahn, W. G. Schmidt, K. Seino, M. Preuss, F. Bechstedt, and J. Bernholc, Phys. Rev. Lett. **94**, 037404 (2005).
[8] Z. Jiangou, Z. Shipin, X. Dingquan, W. Xiu, and X. Guanfeng, J. Phys.: Condens. Matter **4**, 2977 (1992).
[9] D. Redfield and W. J. Burke, J. Appl. Phys. **45**, 4566 (1974).
[10] S. Kase and K. Ohi, Ferroelectrics **8**, 419 (1974).
[11] H. Li, G. Xu, G. Hu, and X. Wang, Cryst. Res. Technol. **29**, 693 (1994).
[12] A. M. Mamedov, M. A. Osman, and L. C. Hajieva, Appl. Phys. A: Solids Surf. **34**, 189 (1984).
[13] E. Wiesendanger and G. Güntherodt, Solid State Commun. **14**, 303 (1974).
[14] V. Caciuc, A. V. Postnikov, and G. Borstel, Phys. Rev. B **61**, 8806 (2000).
[15] M. Veithen and P. Ghosez, Phys. Rev. B **65**, 214302 (2002).
[16] K. Parlinski, Z. Q. Li, and Y. Kawazoe, Phys. Rev. B **61**, 272 (2000).
[17] S. R. Phillpot and V. Gopalan, Appl. Phys. Lett. **84**, 1916 (2004).
[18] I. V. Kityk, M. Makowska-Janusik, M. D. Fontana, M. Aillerie, and F. Abdi, J. Appl. Phys. **90**, 5542 (2001).
[19] F. Bechstedt, in *Festköperprobleme/Advances in Solid State Physics*, edited by U. Rössler (Vieweg, Braunschweig, 1992), Vol. 32, p. 161.
[20] W. Y. Ching, Z.-Q. Gu, and Y.-N. Xu, Phys. Rev. B **50**, 1992 (1994).
[21] S. J. Jenkins, G. P. Srivastava, and J. C. Inkson, Phys. Rev. B **48**, 4388 (1993).
[22] W. G. Schmidt, F. Bechstedt, and G. P. Srivastava, Phys. Rev. B **52**, 2001 (1995).
[23] M. S. Hybertsen and S. G. Louie, Phys. Rev. B **34**, 5390 (1986).
[24] L. J. Sham and T. M. Rice, Phys. Rev. **144**, 708 (1966).
[25] W. Hanke and L. J. Sham, Phys. Rev. B **12**, 4501 (1975).
[26] W. Hanke and L. J. Sham, Phys. Rev. B **21**, 4656 (1980).
[27] G. Kresse and J. Furthmüller, Comput. Mater. Sci. **6**, 15 (1996).
[28] G. Kresse and D. Joubert, Phys. Rev. B **59**, 1758 (1999).
[29] J. P. Perdew, J. A. Chevary, S. H. Vosko, K. A. Jackson, M. R. Pederson, D. J. Singh, and C. Fiolhais, Phys. Rev. B **46**, 6671 (1992).
[30] F. Bechstedt, R. Del Sole, G. Cappellini, and L. Reining, Solid State Commun. **84**, 765 (1992).
[31] J. E. Northrup, Phys. Rev. B **47**, R10032 (1993).
[32] W. G. Schmidt, S. Glutsch, P. H. Hahn, and F. Bechstedt, Phys. Rev. B **67**, 085307 (2003).
[33] P. H. Hahn, W. G. Schmidt, and F. Bechstedt, Phys. Rev. Lett. **88**, 016402 (2001).
[34] H. Boysen and F. Altorfer, Acta Crystallogr., Sect. B: Struct. Sci. **50**, 405 (1994).
[35] I. Inbar and R. E. Cohen, Phys. Rev. B **53**, 1193 (1996).
[36] A. Ridah, M. D. Fontana, and P. Bourson, Phys. Rev. B **56**, 5967 (1997).
[37] A. Ridah, P. Bourson, M. D. Fontana, and G. Malovichko, J. Phys.: Condens. Matter **9**, 9687 (1997).
[38] U. T. Schwarz and M. Maier, Phys. Rev. B **55**, 11041 (1997).
[39] A. S. Barker and R. Loudon, Phys. Rev. **158**, 433 (1967).
[40] M. R. Chowdhury, G. E. Peckham, and D. H. Saunderson, J. Phys. C **11**, 1671 (1978).
[41] Y. Repelin, E. Husson, F. Bennani, and C. Proust, J. Phys. Chem. Solids **60**, 819 (1999).
[42] R. Claus, G. Borstel, L. Steffan, and E. Wiesendanger, Z. Naturforsch. A **27A**, 1187 (1972).
[43] X. C. Yang, G. X. Lan, B. Li, and H. F. Wang, Phys. Status Solidi B **142**, 287 (1987).
[44] F. Bechstedt, K. Seino, P. H. Hahn, and W. G. Schmidt, Phys. Rev. B **72**, 245114 (2005).
[45] R. F. Schaufele and M. J. Weber, Phys. Rev. **152**, 705 (1966).
[46] A. Mansingh and A. Dhar, J. Phys. D **18**, 2059 (1985).